Ray-Tracing Solar Radiation Pressure Modeling for QZS-1 Yaw-Steering Attitude

Francesco Darugna[a,b], Peter Steigenberger[c], Oliver Montenbruck[c], Stefano Casotto[d]

[a] *Università degli Studi di Padova, Department of Industrial Engineering, Via Gradenigo 6/a, 35131 Padova, Italy*
[b] *Geo++ GmbH, Steinriede 8, 30827 Garbsen, Germany*
[c] *Deutsches Zentrum für Luft- und Raumfahrt (DLR), German Space Operations Center (GSOC), Münchener Straße 20, 82234 Weßling, Germany*
[d] *Università degli Studi di Padova, Department of Physics and Astronomy, Vicolo dell'Osservatorio 3, 35122 Padova, Italy*

Abstract

Precise Orbit Determination (POD) requires accurate model for the orbital perturbation. The good knowledge of the gravitational perturbation makes the solar radiation pressure the main perturbative force of global navigation satellite system (GNSS) satellites. The SRP depends on the interaction between the photons of the Sun and the surfaces of the satellite. Hence, a good modeling depends on the geometry and optical properties of the satellite. Previous works showed that the use of a priori box-wing model for the SRP in POD significantly improves the estimated orbit products without a priori model. However, the box-wing model does not consider an accurate geometry. Developing a Computer Aided Design (CAD) model of the QZS-1 satellite of the Quasi Zenith Satellite System (QZSS) a ray-tracing simulation is computed using the commercial software Zemax®. Considering the yaw-steering (YS) attitude of the spacecraft, the results are used to build a ray-tracing model of the SRP for QZS-1. The model is validated considering also complementary empirical parameters based on the empirical CODE Orbit Model (ECOM) formulation in order to include possible deficiencies of the model. Eventually, the ray-tracing model is demonstrated to improve three times the standard deviation of the residuals between estimated QZS-1 orbits and satellite laser ranging residuals with respect to without a priori model. Moreover, the model developed in this work shows an overall better performance than the box-wing model.

Keywords: Solar radiation pressure, ray-tracing model, QZSS, ECOM, Yaw-steering attitude

1. Introduction

Solar radiation pressure (SRP) is the dominant non-gravitational perturbation for global (and regional) navigation satellite systems (GNSSs), that require cm-level orbit knowledge for high-accuracy geodetic applications (Bock and Melgar, 2016). Therefore, Precise Orbit Determination (POD) for GNSSs requires an accurate model for the solar radiation pressure (SRP). Since Earth gravity field and luni-solar gravitational perturbations are well described nowadays, the SRP represents the key objective for accurate prediction and determination for the satellites mentioned above. So far, different kind of SRP models have been developed: models based on ray-tracing and thermal analysis (Ziebart, 2004; Gini, 2014), analytical and semi-analytical models based on generic box-wing models (Rodriguez-Solano et al., 2012) and purely empirical models such as the Empirical CODE Orbit Model (ECOM) (ECOM; Beutler et al., 1994; Springer et al., 1999) and the extended ECOM (ECOM-2; Arnold et al., 2015). Models based on ray-tracing techniques require an accurate description of the geometrical and optical properties of the spacecraft, while a model based on box-wing model considers a simplified geometry of the spacecraft. The ECOM, instead, does not require a priori information, but its performance depends on parameterization. It is important, in fact, to define the correct number of ECOM parameters in order to take into account the properties of the spacecraft so that they are observable.

The deployment of the Quasi-Zenith Satellite System (QZSS; Kogure et al., 2017; Inaba et al., 2009), the Japanese regional navigation satellite system, started in 2010 with its first satellite QZS-1 ("Michibiki"). QZSS broadcasts GPS-compatible signals in order to be an augmentation system for GPS and to provide highly precise and stable positioning services, focusing on the Japanese region. The orbit of QZS-1 is an inclined elliptical geosynchronous orbit used in order to spend a longer time over the Japanese region than over the other regions. In June 2017 QZS-2 was launched and two other satellites, QZS-3 and QZS-4, were launched in August 2017 and October 2017, respectively (Cabinet Office, 2017a). The QZSS service will start in 2018, when three satellites will be visible at all times from locations in the Asia-Oceania regions (Cabinet Office, 2017a). The constellation will be completed in 2023 into a seven-spacecraft constellation using both inclined elliptical geosynchronous and geostationary orbits (Kogure, 2016). Michibiki employs two different attitude modes: the Yaw-Steering (YS) mode and the Orbit-Normal (ON) mode (Ishijima et al., 2009), depending on the elevation of the Sun above the orbital plane (β-angle). In nominal YS mode, $|\beta| > 20°$, the solar panel axis is perpendicular to the Sun and Earth directions and the navigation antenna points towards the Earth (Bar-Sever,

Email addresses: francesco.darugna@geopp.de (Francesco Darugna), peter.steigenberger@dlr.de (Peter Steigenberger), oliver.montenbruck@dlr.de (Oliver Montenbruck), stefano.casotto@unipd.it (Stefano Casotto)

1996). During the ON attitude, $|\beta| < 20°$, the solar panel axis is maintained perpendicular to the orbital plane (Montenbruck et al., 2015a).

QZS-1, as well as Galileo, has an elongated body shape that has to be taken into account, but with respect to Galileo it uses two different attitude modes, as already mentioned. The two attitudes have been investigated through the development of a semi-analytical model based on a box-wing model (Montenbruck et al., 2017a). This model combines an analytic a priori model with a set of five empirical ECOM parameters and it allows to achieve significant improvement with respect to the use of purely empirical models. QZS-1 orbits obtained in this way show, in fact, a better than $10\,\mathrm{cm}$ RMS consistency with SLR measurements; the day boundary discontinuities are reduced by two thirds w.r.t. the orbits obtained without any a priori model; the orbit-clock variations are reduced up to 85% during ON mode. Nevertheless, the use of a box-wing model cannot completely remove orbit errors and empirical SRP parameters. It is especially true in the YS mode, which is the attitude mode most used by the satellite. The performance of a box-wing model as a priori model in POD for QZS-1 has been also investigated in (Zhao et al., 2017). The results of this work show as the augmentation of the ECOM model with an a priori box-wing model can improve the quality of the estimated orbits. In the YS mode, in particular, the RMS of the orbit accuracy by SLR validation results lower than $8\,\mathrm{cm}$ improving the performance without any a priori model of a factor two. Moreover, also the RMS in the ON mode was improved for both the years considered in the analysis (of a factor 3 in the 2014 and of a factor 2 in 2015). Both the previous mentioned works about enhanced SRP models for QZS-1, made assumptions about geometry and optical properties. This is due to the non detailed information available and, therefore, these properties have to be assumed or estimated.

Ray-tracing techniques consider an accurate model of the subject of its analysis. In particular, the spacecraft is represented by a Computer Aided Design (CAD) model which allows to consider all the details of each component of the satellite. For instance, the use of a ray-tracing model in a process of orbit determination considering the satellites GLONASS (Ziebart, 2004) and GOCE (Gini, 2014), improved the quality of the orbits of the spacecrafts. Commercial ray-tracing software is nowadays available, like, for example, OpticStudio-Zemax®[1]. It is an optics analysis software which can implement and solve ray-tracing problems considering CAD geometries and it has already been used to simulate the interaction between the photons of the Sun and the surfaces of the GOCE spacecraft (Gini, 2014).

This paper extends the work described in Montenbruck et al. (2017a). We provide a ray-tracing model of solar radiation pressure for the QZS-1 satellite described by a CAD geometry in YS attitude. Moreover, we furnish a critical comparison with the results obtained with the semi-analytical model presented in Montenbruck et al. (2017a). The reference frames involved in this work, i.e. the YS reference frame and the body-fixed frame, are introduced in Sect. 2. The geometrical and optical properties are described in Sect. 3 taking into account the previous considerations about QZS-1. The ray-tracing approach is analyzed in Sect. 4 together with the implementation of the problem into an optic software. The results of the ray-tracing are used to create the SRP a priori model. In Section 5 the possible improvements of a ray-tracing model are checked in a preliminary analysis. The ray-tracing accelerations are combined with time series of ECOM parameters obtained in QZS-1 orbit determination solutions without a priori model in Sect. 6, showing the results of the POD process.

2. Reference frames

Michibiki employs two different attitude modes: the YS mode and the ON mode. In this work we focus on the YS mode since it is enough to see the improvements that a ray-tracing modeling can offer. Furthermore, the YS mode is less affected by the imbalance of thermal reradiation that cannot be modelled analytically and contributes notable non-gravitational accelerations in ON mode. The unit vectors of the YS reference frame are defined in the following way (Montenbruck et al., 2015a):

$$\begin{aligned} \mathbf{e}_{\mathbf{x},\mathbf{YS}} &= \mathbf{e}_{y,YS} \times \mathbf{e}_{z,YS} \\ \mathbf{e}_{\mathbf{y},\mathbf{YS}} &= \frac{\mathbf{e}_{\odot} \times \mathbf{r}}{|\mathbf{e}_{\odot} \times \mathbf{r}|} \\ \mathbf{e}_{\mathbf{z},\mathbf{YS}} &= -\frac{\mathbf{r}}{|\mathbf{r}|}, \end{aligned} \tag{1}$$

where $\mathbf{e}_{\odot}$ is the unit vector pointing the Sun from the satellite and $\mathbf{r}$ is the satellite position relative to the center of the Earth. For the geometrical analysis the reference frame assumed is the manufacturing frame provided by JAXA, that is different from the body-fixed frame established by the International GNSS Service (IGS) (Montenbruck et al., 2015a).

$$\begin{aligned} \mathbf{e}_{\mathbf{x},\mathbf{BF}} &= -\mathbf{e}_{x,IGS} \\ \mathbf{e}_{\mathbf{y},\mathbf{BF}} &= -\mathbf{e}_{y,IGS} \\ \mathbf{e}_{\mathbf{z},\mathbf{BF}} &= +\mathbf{e}_{z,IGS}. \end{aligned} \tag{2}$$

3. The QZS-1 geometrical and optical properties

The QZS-1 satellite started the QZS constellation in September 2010[2]. As already mentioned its orbit is inclined and geosynchronous with a period of $23^{\mathrm{h}}56^{\mathrm{m}}$ (Montenbruck et al., 2017a). The inclination is about $43°$ and the slight eccentricity to maximize the visibility duration over Japan, is given by: $e = 0.075$. It is a big navigation satellite with an envelope of about $3\,\mathrm{m} \times 3\,\mathrm{m} \times 6\,\mathrm{m}$ and a span of $25\,\mathrm{m}$ (Inaba et al., 2009; JAXA, 2010). Nevertheless there is no published information concerning the size of the different components of the spacecraft. In October 2017 the satellite property information

[1] http://www.zemax.com/os/opticstudio

[2] http://global.jaxa.jp/countdown/f18/index_e.html

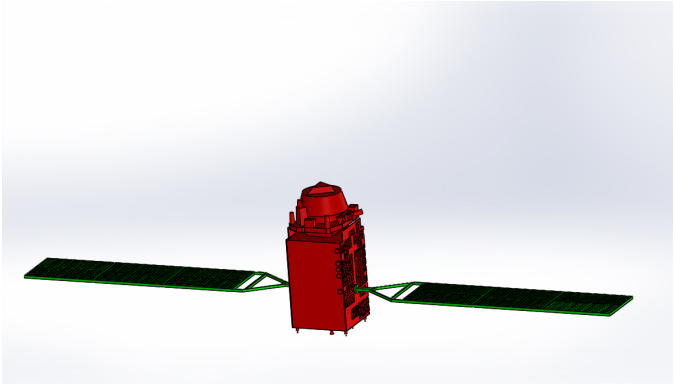

Figure 1: 3D CAD representation of QZS-1

(SPI) and operational history information were published, but without optical properties (they are currently under investigation)(Cabinet Office, 2017b). Since July 2017 the SPI of QZS-2 is available too, but, also in this case, no optical properties have been published. A significant source of information about the dimensions of the satellite was given by a paper-model furnished by the website of JAXA (the website is no more available). With the paper model we can generate a CAD model based on those scaled drawings as shown in Fig. 1. The CAD model is also useful to visualize the geometry of the satellite in the body-fixed frame given by Eq. 2 as can be observed in Fig. 2. The QZS-1 spacecraft is composed of a box-shaped main body with on the side facing the Earth a structure comprising the large L-band GNSS antenna and the other components such as the C-band telemetry, command antennas, retro-reflector array and star trackers. As can be observed, comparing

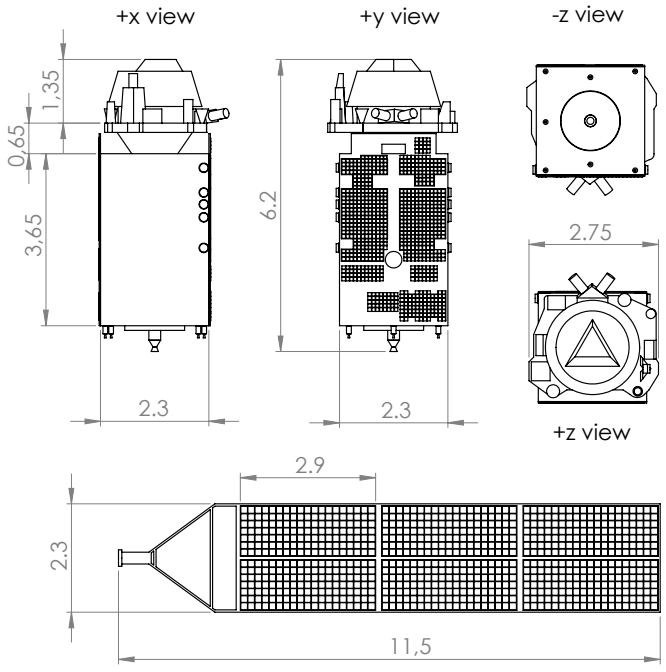

Figure 2: QZS-1 spacecraft geometry and dimensions. All dimensions in [m] and rounded to 5 cm. Reproduced from Montenbruck et al. (2017a).

Fig. 2 and Tab. 1, the geometry computed from the paper model are in a very good agreement with the information provided by the Japanese Cabinet Office. Since there are no published values of the optical properties, they are assumed based on the different materials used for the spacecraft. As already discussed in Montenbruck et al. (2017a) four different kinds of material are considered:

Table 1: Spacecraft dimensions of the spacecraft QZS-1 published in the SPI file (Cabinet Office, 2017b). All values in [m].

Spacecraft element	Dimension
Solar panel	11.45
Body x,y direction	2.35
Body z direction no-thrusters	5.70

- black MLI with a outer carbon-filled layer to prevent electrostatic charging, that will be identified by the name *black*;
- RADOME made from different type of radiofrequency transparent MLI, that will be identified with the name *silver*;
- Mirror-like optical solar reflectors (OSRs), identified with the name *radiator*.

The values of the optical properties assumed for these different surfaces are the same presented in Montenbruck et al. (2017a) and summarized in Tab. 2. The so called black material is a very absorbing material, the radiator material is an almost specular reflective material, while the silver material has a low value of specular reflection.

Table 2: Optical properties of the different material of the body of the spacecraft QZS-1 as assumed in Montenbruck et al. (2017a)

Material	α	δ	ρ
Black	0.94	0.06	0.00
Silver	0.44	0.46	0.10
Radiator	0.06	0.00	0.94

4. Ray-tracing

The ray-tracing approach aims to simulate the interaction between the photons coming from the Sun and the surfaces of the spacecraft. Therefore, it is fundamental to define the geometrical and optical properties of the satellite. The commercial software used to simulate this interaction Sun-satellite through the ray-tracing technique is OpticStudio-Zemax ®, which is further described in 4.2.

4.1. Solar Radiation Pressure

The SRP acceleration is calculated considering two different expressions, i.e. one for the solar panels and another one for

the body of the spacecraft. The reason of this choice stems from consideration of thermal re-emission (Montenbruck et al., 2015b). The expression used for the solar panels is the common one used for the SRP acceleration given by Milani et al. (1987):

$$\boldsymbol{a} = -\frac{\Phi}{mc} A \cos\theta \cdot \left[(\alpha + \delta)\boldsymbol{e}_{\odot} + \frac{2}{3}\delta \boldsymbol{e}_n + 2\rho \cos\theta \boldsymbol{e}_n \right], \tag{3}$$

where A is the surface involved in the interaction, $\boldsymbol{e}_n$ is the unit vector perpendicular to the surface A, θ is the angle between the normal of the surface impinged by the ray and the ray itself, α, δ and ρ are respectively the coefficients of the absorbed, diffusely and specularly reflected fraction of the incident radiation. For the body of the spacecraft, instead, is considered also an almost instantaneous re-radiation of the absorbed radiation. In terms of acceleration it means (**?**):

$$\boldsymbol{a} = -\frac{\Phi}{mc} \cdot A \cos\theta \cdot \left[\frac{2}{3}\alpha \boldsymbol{e}_n \right]. \tag{4}$$

Therefore, considering the above mentioned contribution, the equations for the SRP acceleration for the body yields:

$$\boldsymbol{a} = -\frac{\Phi}{mc} A \cos\theta \cdot \left[(\alpha + \delta)(\boldsymbol{e}_{\odot} + \frac{2}{3}\boldsymbol{e}_n) + 2\rho \cos\theta \boldsymbol{e}_n \right], \tag{5}$$

The use of these equations underlines the need of an accurate knowledge of geometrical and optical properties of all the components of the satellite as well as the identification of all the surfaces involved in every different configuration Sun-satellite. Specific requirements include:

- an accurate description of the geometry;
- an accurate description of the optical properties of all the components of the satellite;
- to identify all the rays that impinge the spacecraft, hence the direction of the rays in all the different configurations Sun-satellite;
- to define the normal to the surfaces impinged by the radiation in different relative configurations Sun-satellite.

In the following paragraphs all the aforementioned points are carried out.

4.2. Zemax

Zemax is an optic software with several possible applications in the field of physics and, in particular, in the branch of optics. It allows to import CAD files describing the geometry of the object, to define a proper source of rays of light and to simulate the interaction between the two. Hence, once defined the CAD file of the spacecraft it is imported into the Zemax environment as the object of the ray-tracing. The solar illumination is considered as a parallel beam of light with rectangular cross-section, whose sides are longer than the longest dimension of the satellite. A defined number of rays start from the source and impinge the surfaces of the spacecraft as shown in Fig. 3. The rectangular source is modelled as a grid of pixels with a resolution that can be set. In this particular case the chosen source of rays is a quadratic grid with the following characteristics:

- dimensions: $26\,\mathrm{m} \times 26\,\mathrm{m}$;

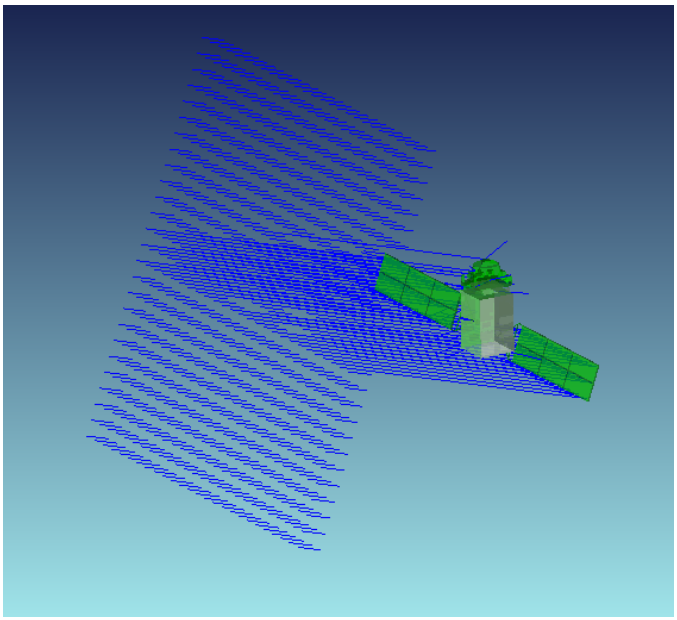

Figure 3: Simulation of the problem in Zemax.

- a resolution of $0.1\,\mathrm{m} \times 0.1\,\mathrm{m}$.

Hence, the grid, representing the light source, is divided into 67600 pixels of dimensions $0.1\,\mathrm{m} \times 0.1\,\mathrm{m}$. From the center of each pixel a ray starts towards the spacecraft. In order to simulate the interaction Sun-satellite Zemax needs a description of the relative Sun-satellite configuration. It consists in a macro function of Zemax which contains the description of the relative configuration. Since only the YS mode is considered, the Sun lies in the x-z plane of the spacecraft (Montenbruck et al., 2015b) and it rotates with an angle, called azimuth angle *Az*, around the satellite. The azimuth angle stays in the interval $Az \in [0,360]^{\circ}$ and it is defined with a stepsize of 1°. Moreover, Zemax allocates an identification number (ID number) to each surface of each component of the spacecraft. The simulation in Zemax considers also multiple reflections. A multiple reflection is considered when the specularly reflected fraction of a ray which has impinged a surface, then it impacts another surface of a component of the satellite. The number of multiple reflections is empirically set to three considering the effective contribution of an amount which is pretty low also looking at the values of the optical coefficients of the materials involved (Tab. 2). The output of Zemax is given by:

- the $\boldsymbol{e}_{\odot,i}$ for each i^{th} ray that impinges the spacecraft;
- the $\boldsymbol{e}_{n,i}$ of each surface impinged by the i^{th} ray;
- the ID number of each surface of each component of the spacecraft impinged by the i^{th} ray.

In other words, the ray-tracer identifies all the surfaces impinged by the rays and it associates them to a particular relative configuration Sun-satellite, computing the unit vector of the spacecraft-Sun direction and that one of the normal to the surface impinged for all the surfaces involved in that configuration. Therefore, now, there are all the elements to compute the SRP acceleration. This step is developed using another software: the Aerodynamics and Radiation Pressure Analysis (ARPA) devel-

oped at the University of Padua (Gini, 2014).

4.3. ARPA

ARPA is a software which computes forces and torques on a satellite due to non-gravitational perturbations, such as solar radiation pressure, Earth radiation pressure, the satellite thermal re-radiation and the aerodynamics (Gini, 2014). For the purpose of this work it is used to compute the SRP acceleration since the thermal properties and behaviour are not accurately defined by the published information. The software reads the output of the ray-tracer of Zemax, that is a binary file, and it calculates the force due to the solar radiation pressure. Every surface of the spacecraft, identified by the ID number which Zemax set, is associated to the corresponding set of optical properties considering the material which covers it (Tab. 2). The SRP force is computed as the sum of the contribution of every pixel. To each pixel corresponds, in fact, a contribution of the force that is zero if the ray starting from the center of that particular pixel does not impinge the satellite. The sum of the contribution of each pixel gives the total force for a particular relative configuration Sun-spacecraft. The expression of the force associated to a ray which impacts a surface of the satellite is given by:

$$\boldsymbol{F} = -F_{pixel} \cdot \boldsymbol{F}_{op}, \tag{6}$$

where:

$$F_{pixel} = \frac{\Phi A \cos\theta}{c} = \frac{\Phi A_{pixel}}{c}, \tag{7}$$

with A_{pixel} corresponding to the surface of the pixel, i.e. $1\,\mathrm{dm}^2$. The vector $\boldsymbol{F}_{op}$, instead, depends on the surface involved: solar panels or body of the spacecraft as can be deduced from Eqs. 3, 5. In fact if the surface impinged belongs to the solar panels:

$$\boldsymbol{F}_{op} = (\alpha + \delta)\boldsymbol{e}_\odot + \frac{2}{3}\delta\boldsymbol{e}_n + 2\rho\cos\theta\boldsymbol{e}_n. \tag{8}$$

While if the surface belongs to the body it results:

$$\boldsymbol{F}_{op} = (\alpha + \delta)(\boldsymbol{e}_\odot + \frac{2}{3}\boldsymbol{e}_n) + 2\rho\cos\theta\boldsymbol{e}_n. \tag{9}$$

As already mentioned, in this work we consider also multiple reflections and ARPA can manage them. The result is that the force per pixel associated to each specularly reflected ray after the n-th reflection is given by (Gini, 2014):

$$F_{\text{pixel-n}^{\text{th}}\text{reflection}} = \frac{\Phi A_{pixel}}{c}\prod_{j=i}^{N}\rho_j. \tag{10}$$

Hence, for each relative configuration Sun-satellite defined, considering the YS mode, by the azimuth angle *Az*, ARPA computes the force due to the solar radiation pressure perturbation by summing the effect associated to every pixel of the ray-source grid. The output of ARPA is a table with the three components of the force in the *x*, *y*, *z* directions for each angle *Az*. However, to implement such a model in an orbit determination process, the value of the force is needed for any values of *Az* and not only for the tabulated values. This problem is easily solved considering a linear interpolation process. Eventually, the acceleration is computed considering the mass of the spacecraft, evaluated as dry mass plus a residual fuel for orbit-keeping and end-of-life operations: $m = 2000\,\mathrm{kg}$ (Montenbruck et al., 2017a).

5. Preliminary analysis

The SRP acceleration computed from the output of ARPA represents the ray-tracing model. This has to be validated in a precise orbit determination process in order to analyze the effective benefits that it can provide. First, however, there are some considerations to take into account: the contribution of the solar panels and the difference with respect to a box-wing model.

5.1. The impact of the solar panels

The solar panels and the body of the QZS-1 satellite have different relative position with respect to the Sun. The solar panels, in fact, are always kept perpendicular to the Sun-direction during the YS mode, while the body does not rotate. Therefore, it is interesting to consider the two as different bodies in different simulations. Accordingly, two problems have been investigated with the ray-tracing technique. The sum of the SRP acceleration obtained considering the two objects taken individually is compared with that one which results by considering the complete spacecraft. In this way the importance of the multiple reflections between the solar panels and the body of the spacecraft are studied. The simulations show that the RMS difference of the two cases amounts to $1\,\mathrm{nm/s}^2$. This value is not so big considering the total amount of the acceleration of roughly $156\,\mathrm{nm/s}^2$. However, $1\,\mathrm{nm/s}^2$ is the order of magnitude of the ECOM parameters obtained with the a priori box-wing model developed in the previous work and it is something that has to be taken into account.

5.2. Comparison with box-wing model

A preliminary analysis considering the best box-wing which fits the ray-tracing results can suggest if the employment of a ray-tracing model could really improve what obtained with a box-wing model. For this purpose is considered the satellite without solar panels. It founds reason in the fact that the solar panels add uncertainty in the results. The assumptions made for the optical properties of the panels are, in fact, even more strong than those made on the body of the spacecraft. The box-wing model considered is defined by only two parameters: $a_z^{\alpha\delta}$ and $a_x^{\alpha\delta}$. These two characteristic accelerations are expressed in order to take into account the symmetric contributions of the $\pm$z and $\pm$x. The RMS of the fit of this analytical model to the ray-tracing model, obtained with a least squares approach, is roughly $1\,\mathrm{nm/s}^2$ (RMS=$1.01\mathrm{nm/s}^2$). It is a low value considering the total amount of the SRP, i.e. roughly the 4% (without solar panels). Nevertheless, considering the difference of the two models as the SRP model in a orbit determination process, the little gap causes not negligible results. Furthermore, as can

be noticed, the RMS is comparable with the results obtained in the previous subsection. Eventually, it is interesting that there is a proper box-wing model which can fit the ray-tracing results and that this model is very similar to the adjusted box-wing model proposed in Montenbruck et al. (2017a). As can be

Table 3: Characteristic accelerations of the box-wing model in two different cases: the adjusted model of Montenbruck et al. (2017a) and the model fitted to the ray-tacing results. All values in $\mathrm{nm/s^2}$.

Acceleration	adjusted model	fitted model
$a_z^{\alpha\delta}$	13.00	13.13
$a_x^{\alpha\delta}$	27.00	28.31

observed from Tab. 3, the values of the parameters of the two models are comparable and they differ, at most, a little more than $1\,\mathrm{nm/s^2}$. This analysis does not deal with real observation, it has the purpose to understand if the difference between a simplified model and a more accurate model implies significant results concerning the radial residuals and the values of the empirical parameters.

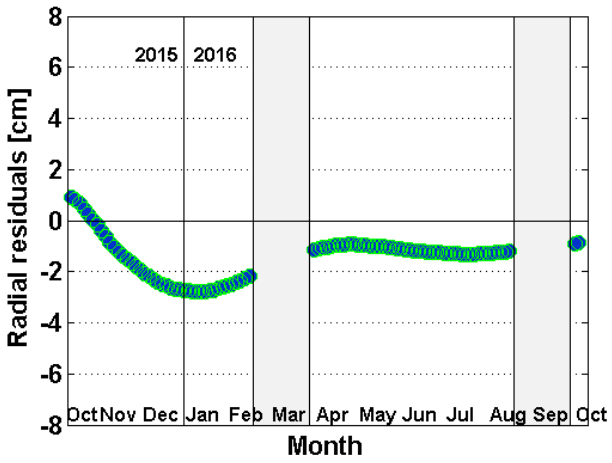

Figure 4: Radial residual considering the difference between the ray-tracing model and the box-wing model which best fits the ray-tracing results as SRP model in an orbit determination process. The period of time considered is from October 2015 to October 2016. The shaded areas represent the Orbit Normal mode.

Figure 4 shows the effect in radial residuals, obtained as the difference in the radial direction between an orbit propagated without a priori SRP model and that one considering the aforementioned difference as SRP model. The radial residuals vary in the interval [0;3]cm in absolute value. It is a magnitude not negligible for a POD which aims to achieve high performance. It suggests that to consider a more accurate model, such as a ray-tracing model, could potentially improve the quality of the estimated orbits. Moreover, considering the ECOM parameters, the results of this analysis are comparable with those ones obtained with the adjusted box-wing model described in (Montenbruck et al., 2017a). It means that the ray-tracing model could, completely or in part, explain the presence of empirical acceleration using an a priori model, as the simplified box-wing model.

6. Model Validation

GPS and QZSS observations of network of 130 stations have been processed with the NAPEOS v3.3.1 software package (Agueda and Zandbergen, 2004) for the time interval 3 January 2015 until 17 December 2016. Most stations are multi-GNSS stations provided by the Multi-GNSS Experiment (MGEX, Montenbruck et al., 2017b) of the IGS (Dow et al., 2009; IGS, 2017). Depending on the time, 30 – 55 stations offer QZS-1 tracking capability. In addition, legacy IGS stations have been considered in order to densify the tracking network in areas with sparse coverage. The ionosphere-free linear combination of L1 and L2 is used for both, GPS and QZSS. The estimation parameters for each 3-day orbital arc include station coordinates, troposphere zenith delays, Earth rotation parameters, receiver and transmitter clock offsets, inter-system biases, as well as orbital parameters. Ambiguities are only fixed for GPS with the Melbourne Wuebbena approach (Melbourne, 1985; Wübbena, 1985). More details on the GNSS data processing are given in Table 2 of Montenbruck et al. (2017a) but the IGS14 reference frame (Rebischung et al., 2016a) and the igs14.atx antenna model (Rebischung et al., 2016b) have been used in the current work. Three solutions with different orbit modeling for QZS-1 have been computed:

- 5-parameter ECOM (without a priori model)
- a priori box-wing model + 5-parameter ECOM (macro model)
- a priori ray-tracing model + 5-parameter ECOM

Figure 5 shows the estimated ECOM parameters for the solutions without a priori model and with a priori ray-tracing model. In the ray-tracing model the contribution of the solar panels has been considered with a value of $-115\,\mathrm{nm/s^2}$. The value for the solar panels was estimated empirically starting from the geometrical and optical assumption of Table 1 of Montenbruck et al. (2017a). A mean value of D_0= $-157.5\,\mathrm{nm/s^2}$ has been subtracted for the solution without a priori model.

As can be observed from Fig 5 the $|\beta|$ dependency of the ECOM parameters is significantly reduced applying the a priori ray-tracing model in the YS mode. The amplitude of the ECOM D_0 parameters is reduced from $4\,\mathrm{nm/s^2}$ to less than $1\,\mathrm{nm/s^2}$. While the box-wing model does not affect the modeled acceleration, the ray-tracing model has an impact also in this direction. Both the dependency on the β-angle and the amplitude of the ECOM Y_0 are, in fact, decreased close to zero. The amplitude of roughly $1\,\mathrm{nm/s^2}$ of Y_0 in the proximity of the border of the ON mode is lower than the half with the ray tracing model applied.

The curved shape of the contribution of the ECOM B_0 parameters cannot be removed even considering a ray-tracing model. Nevertheless, the overall amplitude of this parameter is reduced from an interval between $1\,\mathrm{nm/s^2}$ and $2\,\mathrm{nm/s^2}$ to values lower than $1\,\mathrm{nm/s^2}$. Moreover, the asymmetry between negative and positive values decreases when the ray-tracing model is taken into account. The systematic effects for B_C^* and

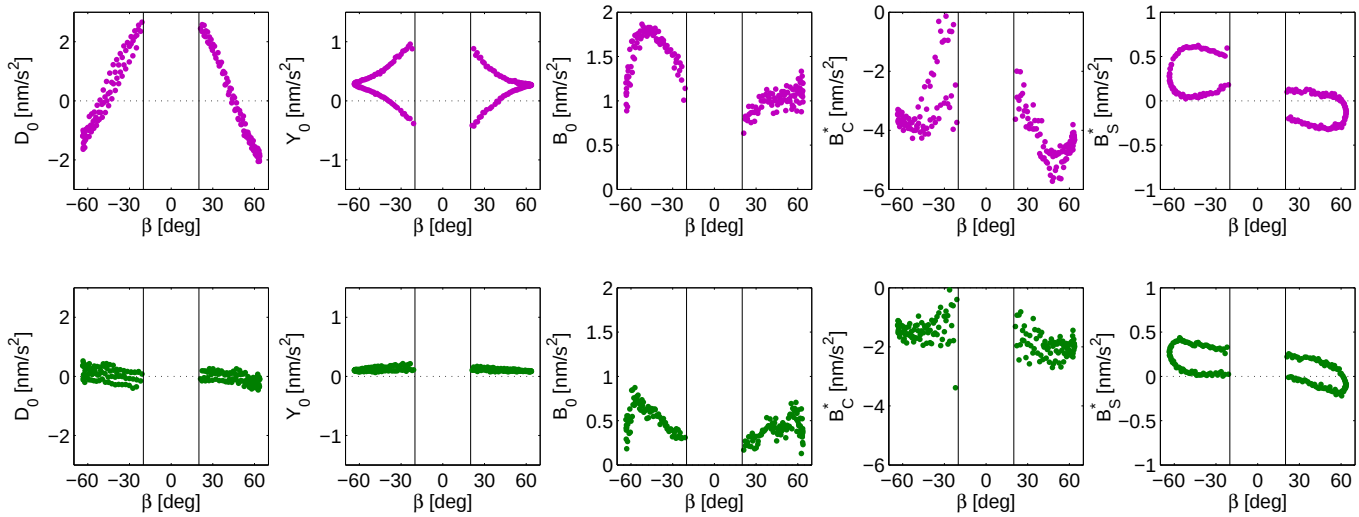

Figure 5: Estimated ECOM parameters: no a priori model (top), a priori ray-tracing model (bottom).

Table 4: Day boundary discontinuities and RMS 3-day orbit predictions w.r.t. orbit arcs based on observations. Only time intervals with YS-mode are considered.

Solution	DBD [cm]	Pred. [cm]
5-par. ECOM	70	177
Macro Model	35	56
Ray-Tracing	19	51

Table 5: Offset and standard deviation (STD) of QZS-1 SLR residuals. Only time intervals with YS-mode are considered.

Solution	Offset [cm]	STD [cm]
5-par. ECOM	−4.2	14.8
Macro Model	−1.6	7.2
Ray-Tracing	−8.9	4.5

B_S^* are considerably reduced and also the hysteresis decreased. Therefore, as in the case of the box-wing model (Montenbruck et al., 2017a), the application of an a priori model has a significant positive effect on the reduction of the estimated ECOM parameters. Furthermore, the ray-tracing model achieves a better performance than the box-wing model in terms of magnitude of the reduction.

Day-boundary discontinuities (DBDs) are a measure for the internal consistency of satellite orbits. They are computed as 3D difference of the orbit positions of two consecutive arcs at midnight. Mean values for the DBDs are listed in the left part of Table 4. The macro model reduces the DBDs by a factor of two compared to the 5-parameter ECOM. Introducing the ray-tracing model results in DBDs less than two decimeter, another improvement of a factor of almost two compared to the macro model.

Another internal quality indicator is the orbit prediction performance: an orbit prediction covering three days is compared with a 3-day arc completely obtained from observations. Resulting mean RMS values for the analyis interval limited to time periods with YS-mode are listed in the right part of Table 4. The performance of macro and ray-tracing model does not differ significantly for the orbit prediction RMS. However, both values are with about half a meter smaller by a factor of three compared to the solution without a priori model.

The *accuracy* of the estimated satellite orbits can be evaluated by the independent (optic) satellite laser ranging (SLR) technique. Five SLR stations of the International Laser Ranging Service (Pearlman et al., 2002, ILRS) track QZS-1 on a regular basis: Beijing, Changchun, and Shanghai in China as well as Mount Stromlo and Yarragadee in Australia. For the total analysis interval, 2686 normal points are available. If only the YS-mode is considered, the normal point number is 1997. Station coordinates are fixed to SLRF2014[3] and observations below 10° or exceeding an outlier limit of $1\,\mathrm{m}$ are excluded. Offset and standard deviation (STD) of the SLR residuals are listed in Table 5 for the three solutions. Time series of the two solutions with different a priori models are plotted in Fig. 6. The macro model improves the STD of the SLR residuals by a factor of two, the absolute value of the SLR bias is reduced by $2.6\,\mathrm{cm}$. Switching to the ray-tracing model results in a further reduction of the SLR residuals to $4.5\,\mathrm{cm}$, i.e., an improvement by about one third. However, the SLR offset increases to about $9\,\mathrm{cm}$. The origin of this offset is unknown. Steigenberger et al. (2015) showed that not modeling an additional plate carrying the laser retroreflector of GIOVE-B introduces an SLR offset of almost $10\,\mathrm{cm}$. Small-scale strucures of the satellite not covered by the current ray-tracing model might explain the $-9\,\mathrm{cm}$ bias.

[3]available at ftp://cddis.nasa.gov/slr/products/resource

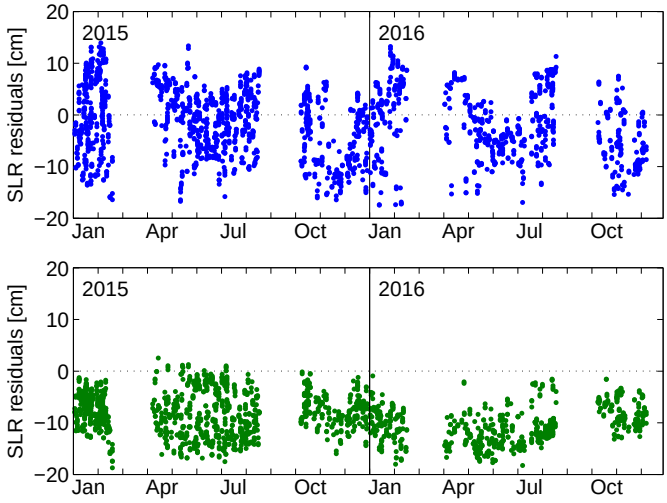

Figure 6: SLR residuals during YS-mode: a priori model box-wing model (top), a priori ray-tracing model (bottom).

7. Summary and Conclusion

Using the commercial software Zemax® a ray-tracing simulation of the interaction between the solar photons and the surfaces of the components of the QZS-1 satellite during the YS mode was computed. The ARPA software of the University of Padua calculated the SRP acceleration from the Zemax output of the ray-tracing simulation. In this way, tables of the SRP acceleration were filled as function of the azimuth angle A_z. The spacecraft during the ray-tracing simulation was represented by a CAD model based on a paper model whose geometric properties are in very good agreement with the published dimensions. The ray-tracing model has been carried out without considering the solar panels, because of the big uncertainty about the optical properties. A preliminary analysis showed the possibility of an improvement in the quality of estimated orbits considering a ray-tracing model for the body of the satellite w.r.t. a box-wing model. The benefits of the application of a ray-tracing model in the quality of the estimation of the orbit has been presented in terms of the SLR residuals, day boundary discontinuities and RMS 3-day orbit predictions. With respect to the box-wing model, the ray-tracing model provides an improvement of 16 cm in day boundary discontinuities, of 5 cm in the RMS of the 3-day orbit predictions and roughly an improvement of 3 cm in the STD of the SLR residuals. However, the application of the ray-tracing model increased the offset of the SLR residuals to about 9 cm. The source of this bias is still unknown, but could be explained by small-scale structures of the satellite not covered by the current ray-tracing model.

With the exception of the SLR bias, the ray-tracing model improve the quality of the estimated orbits with the box-wing model. Nevertheless, even using this accurate geometric model both orbit errors and the empirical ECOM parameters can be completely removed. Further improvements and, maybe, also the explanation of the 9 cm of SLR offset could be achieved with a complete ray-tracing model with the real optical properties of the surfaces of the satellite. Moreover, with information about the thermal properties a thermal re-radiation pressure analysis could be provided by the ARPA software. However, the publication of optical and thermal properties by the Cabinet Office is still pending.

Acknowledgments

The Multi-GNSS Pilot Project (MGEX) of the International GNSS Service (IGS) and the International Laser Ranging Service (ILRS) are acknowledged for providing multi-GNSS and SLR observation data. We also thank the European Space Agency for granting access to the NAPEOS v3.3.1 software used in this study.

References

Agueda, A., Zandbergen, R., 2004. NAPEOS mathematical models and algorithms. Tech. Rep. NAPEOS-MM-01, iss. 3.0, 04/06/2004, ESA/ESOC, Darmstadt.

Arnold, D., Meindl, M., Beutler, G., Dach, R., Schaer, S., Lutz, S., Prange, L., Sosnica, K., Mervart, L., Jggi, A., 2015. CODE's new solar radiation pressure model for GNSS orbit determination. Journal of Geodesy 89 (8), 775–791.

Bar-Sever, Y. E., 1996. A new model for GPS yaw attitude. J. Geod. 70 (11), 714–723, DOI 10.1007/BF00867149.

Beutler, G., Brockmann, E., Gurtner, W., Hugentobler, U., Mervart, L., Rothacher, M., Verdun, A., 1994. Extended orbit modeling techniques at the CODE processing center of the International GPS Service for Geodynamics (IGS): Theory and initial results. Manuscr. Geod. 19 (6), 367–386.

Bock, Y., Melgar, D., 2016. Physical applications of GPS geodesy: a review. Reports on Progress in Physics 79 (10), 106801.

Cabinet Office, 2017a. Quasi-zenith satellite system. URL http://qzss.go.jp/en/index.html

Cabinet Office, 2017b. QZS-1 satellite information. Tech. Rep. SPI_QZS1, Government of Japan, National Space Policy Secretariat. URL http://qzss.go.jp/en/technical/qzssinfo/index.html

Dow, J. M., Neilan, R. E., Rizos, C., 2009. The International GNSS Service in a changing landscape of Global Navigation Satellite Systems. J. Geod. 83 (3-4), 191–198, DOI 10.1007/s00190-008-0300-3.

Gini, F., 2014. GOCE precise non-gravitational force modeling for POD applications. Ph.D. thesis, Università degli Studi di Padova.

IGS, 2017. Daily 30-second observation data, NASA Crustal Dynamics Data Information System (CDDIS). DOI 10.5067/GNSS/gnss_daily_o_001.

Inaba, N., Matsumoto, A., Hase, H., Kogure, S., Sawabe, M., Terada, K., 2009. Design concept of Quasi Zenith Satellite System. Acta Astronaut. 65 (7), 1068–1075, DOI 10.1016/j.actaastro.2009.03.068.

Ishijima, Y., Inaba, N., Matsumoto, A., Terada, K., Yonechi, H., Ebisutani, H., Ukava, S., Okamoto, T., 2009. Design and developement of the first Quasi-Zenith Satellite attitude and orbit control system. In: 2009 IEEE Aerospace Conference. IEEE, pp. 1–8, DOI 10.1109/AERO.2009.4839537.

JAXA, 2010. Presskit first Quasi-Zenith Satellite System MICHIBIKI. URL http://global.jaxa.jp/countdown/f18/pdf/presskit_michibiki_e.pdf

Kogure, S., 2016. Status update on the Quasi-Zenith Satellite System. In: ICG-11,Sochi, Russian Federation.

Kogure, S., Ganeshan, A. S., Montenbruck, O., 2017. Regional systems. In: Teunissen, P. G., Montenbruck, O. (Eds.), Springer Handbook of Global Navigation Satellite Systems. Springer, Ch. 11, pp. 305–337, DOI 10.1007/978-3-319-42928-1_11.

Melbourne, W. G., 1985. The case for ranging in GPS based geodetic systems. In: Goad, C. (Ed.), Proceedings of the First International Symposium on Precise Positioning with the Global Positioning System. U.S. Department of Commerce, Rockville, Maryland, pp. 373–386.

Milani, A., Nobili, A. M., Farinella, P., 1987. Non-gravitational Perturbations and Satellite Geodesy. Adam Hilger Ltd., Bristol, UK.

Montenbruck, O., Schmid, R., Mercier, F., Steigenberger, P., Noll, C., Fatkulin, R., Kogure, S., Ganeshan, A. S., 2015a. GNSS satellite geometry and attitude models. Adv. Space Res. 56 (6), 1015–1029, DOI 10.1016/j.asr.2015.06.019.

Montenbruck, O., Steigenberger, P., Darugna, F., 2017a. Semi-analytical solar radiation pressure modeling for QZS-1 orbit-normal and yaw-steering attitude. Adv. Space Res. 59 (8), 2088–2100.

Montenbruck, O., Steigenberger, P., Hugentobler, U., 2015b. Enhanced solar radiation pressure modeling for Galileo satellites. J. Geod. 89 (3), 283–297, DOI 10.1007/s00190-014-0774-0.

Montenbruck, O., Steigenberger, P., Prange, L., Deng, Z., Zhao, Q., Perosanz, F., Romero, I., Noll, C., Stürze, A., Weber, G., Schmid, R., MacLeod, K., Schaer, S., 2017b. The Multi-GNSS Experiment (MGEX) of the International GNSS Service (IGS) - achievements, prospects and challenges. Adv. Space Res. 59 (7), 1671–1697.

Pearlman, M., Degnan, J., Bosworth, J., 2002. The International Laser Ranging Service. Adv. Space Res. 30 (2), 125–143, DOI 10.1016/S0273-1177(02)00277-6.

Rebischung, P., Altamimi, Z., Ray, J., Garayt, B., 2016a. The IGS contribution to ITRF2014. J. Geod. 90 (7), 611–630, DOI 10.1007/s00190-016-0897-6.

Rebischung, P., Schmid, R., Herring, T., 2016b. [IGSMAIL-7399] upcoming switch to IGS14/igs14.atx.
URL https://lists.igs.org/pipermail/igsmail/2016/001233.html

Rodriguez-Solano, C., Hugentobler, U., Steigenberger, P., 2012. Adjustable box-wing model for solar radiation pressure impacting gps satellite. Adv Space Res 49 (7), 1113–1128.

Springer, T., Beutler, G., Rothacher, M., 1999. A new solar radiation pressure model for GPS satellites. GPS Solut. 2 (3), 50–62, DOI 10.1007/PL00012757.

Steigenberger, P., Montenbruck, O., Hugentobler, U., 2015. GIOVE-B solar radiation pressure modeling for precise orbit determination. Advances in Space Research 55 (5), 1422–1431.

Wübbena, G., 1985. Software developments for geodetic positioning with GPS using TI-4100 code and carrier measurements. In: Goad, C. (Ed.), Proceedings of the First International Symposium on Precise Positioning with the Global Positioning System. U.S. Department of Commerce, Rockville, Maryland, pp. 403–412.

Zhao, Q., Chen, G., Guo, J., Liu, J., Liu, X., 2017. An a priori solar radiation pressure model for the QZSS Michibiki satellite. J. Geod.DOI 10.1007/s00190-017-1048-4.

Ziebart, M., 2004. Generalized analytical solar radiation pressure modeling algorithm for spacecraft of complex shape. J. Spacecr. Rockets 41 (5), 840–848, DOI 10.2514/1.13097.